The Tribological Characteristics of Phosphorylated 3-Aminopropyltriethoxysilane Nanometer Film

J. Li,[1] X. Z. Li[2]

[1]*School of Mechanical and Electronic Engineering, Shanghai Second Polytechnic University, Shanghai 201209, People's Republic of China*
[2]*English Group, Shouguang Experimental School, Shandong Shouguang 261041, People's Republic of China*

Received 12 September 2008; accepted 1 November 2008
DOI 10.1002/app.29618
Published online 23 February 2009 in Wiley InterScience (www.interscience.wiley.com).

ABSTRACT: Thin films deposited on the phosphonate 3-aminopropyltriethoxysilane (APTES) self-assembled monolayer (SAM) were prepared on the hydroxylated silicon substrate by a self-assembling process from specially formulated solution. Chemical compositions of the films and chemical state of the elements were detected by X-ray photoelectron spectrometry. The thickness of the films was determined with an ellipsometer, whereas the morphologies and nanotribological properties of the samples were analyzed by means of atomic force microscopy. As the results, the target film was obtained and reaction may have taken place between the thin films and the silicon substrate. It was also found that the thin films showed the lowest friction and adhesion followed by APTES-SAM and phosphorylated APTES-SAM, whereas silicon substrate showed high friction and adhesion. Microscale scratch/wear studies clearly showed that thin films were much more scratch/wear resistant than the other samples. The superior friction reduction and scratch/wear resistance of thin films may be attributed to low work of adhesion of nonpolar terminal groups and the strong bonding strength between the films and the substrate. © 2009 Wiley Periodicals, Inc. J Appl Polym Sci 112: 2641–2646, 2009

Key words: thin films; friction; adhesion; scratch/wear

INTRODUCTION

Microelectromechanical systems (MEMS) and emerging nanoelectromechanical systems (NEMS) are expected to have a major impact on our lives, much like the way that the integrated circuit has affected information technology.[1,2] However, due to the large surface area to volume to volume ratio in MEMS/NEMS devices as the size scale shrinks, currently many potential applications for MEMS/NEMS are not really practical, as many studies have revealed the profound negative influence of stiction, friction, and wear on the efficiency, power output, and steady-state speed of micro/nanodynamic devices.[3–6] The self-assembled monolayer (SAM) has gained growing interest over the past years because it has advantageous characteristics of well-defined structure, strong head group-substrate binding, and dense packing of hydrocarbon chains. Indeed SAM considerably reduces friction and adhesion and is found use in various MEMS devices.[7–11]

Correspondence to: X. Z. Li (lishuyang2003.student@sina.com).

Contract grant sponsor: Shanghai Second Polytechnic University; contract grant number: JD208001.

A number of studies have been done on the nanotribological properties of different SAMs,[12,13] but the study of the rare earth films on the nanotribological behavior is still much lacking. In this study, thin films deposited on the phosphorylated APTES-SAM were prepared on the silicon substrates. X-ray photoelectron spectroscopy (XPS), atomic force microscopy (AFM), ellipsometer, and contact angle measurements were applied to investigate the structure and nanotribological properties of the prepared films.

EXPERIMENTAL

Preparation of thin films on the phosphorylated APTES-SAM

APTES was purchased from Aldich Chemical Company, Inc. A single-crystal silicon wafer polished on one side was used as substrate for the SAM transfer. Other reagents were of analytical grade. Deionized water was used throughout the experiment. For the preparation of the target solution, APTES, toluene, ethanol, acetonitrile, phosphorus oxychloride, and collidine were commercially obtained and used without further purification. The silicon substrates were cleaned with "piranha" solution [$H_2SO_4 : H_2O_2 = 7 : 3$ ($v : v$); caution: this solution reacts violently with organics], then exposed to a solution of APTES in toluene (2% $v : v$, 24 h, room temperature), followed by

$POCl_3$ in acetonitrile (0.2*M* $POCl_3$, 0.2*M* collidine, 20 min, room temperature), according to the described procedure.[14,15] This treatment resulted in surface rich in phosphonate groups ($-PO(OH)_2$), which adsorbed a layer of thin films when immersed in preprepared solution, then naturally cooled in a desiccator. To help the reader for better understanding, schematic of growth of thin films on phosphorylated APTES-SAM is shown in Figure 1.

Description of apparatus and test procedures

Chemical compositions of the films and chemical state of the elements were analyzed by a PHI-5702 XPS system, using Mg-Kα radiation operating at 250W and pass energy of 29.35 eV. The binding energy of C 1s (284.6 eV) was used as the reference. The resolution for the measurement of the binding energy is about ±0.3 eV. The static contact angles were measured in ambient air (relative humidity 40%) using an OCA-20 contact angle measurement device (DataPhysics Instruments Gmbh, Germany). Distilled water was used as the spreading reagent. Measurements were performed on at least three samples, and were made at a minimum of three different spots on each sample. The contact angles were typically reproducible to within ±2°. The thickness of the films was measured on an ellipsometer (V-VASE with AutoRetarder from J.A. Woollam Co., polarizer-retarder-sample-rotating analyzer configuration) which was equipped with a He-Ne laser (632.8 nm) set an incident angle of 70°. The index of refraction for the refraction was taken to be 1.45. Thickness data were obtained by averaging five measurements at different spots of each sample surface. The thickness was recorded to an accuracy of ±0.3 nm.

The surface morphology and the nanotribological properties of the prepared films were investigated using an SPM-9500 atomic force microscope (NanoScope IIIa) produced by Shimadzu Corporation (Kyoto, Japan). Square pyramidal Si_3N_4 tips with a nominal 50 nm radius mounted on gold-coated triangular Si_3N_4 cantilevers with spring constants of 0.6 N/m were used. The adhesion and friction data were measured at 10 times at each interesting location and average data values were obtained. Adhesive forces were measured using the so called "force calibration plot." Friction forces were measured also according to Ref. 16. By following the friction force calibration procedures developed by Bhushan,[17] voltages corresponding to friction forces can be converted to force units. Coefficient of friction is obtained from the slope of friction force data measured as a function of normal loads.

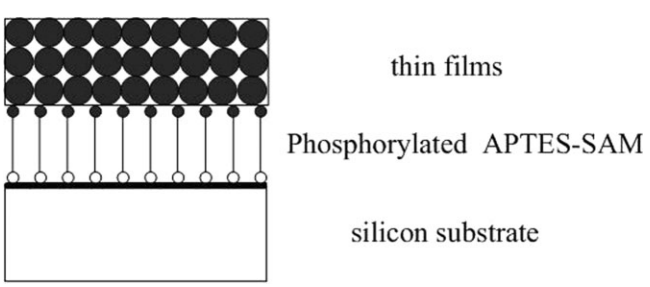

Figure 1 Schematic of growth of thin films on phosphorylated APTES-SAM.

For the scratch and wear tests, specially fabricated microtips were used. These microtips consisted of single-crystal natural diamond, ground to the shape of a three-sided pyramid, with an apex angle of 80° and tip radius of about 50 nm, mounted on a platinum-coated stainless steel cantilever beam whose stiffness was 50 N/m. Samples were scanned orthogonal to the long axis of the cantilever with loads ranging from 20 to 100 μN to generate scratch/wear marks. Observations of the sample surface before and after the wear tests were done by scanning parallel to the long axis of the cantilever with loads ranging from 0.5 to 1 μN. The parallel scans enabled near-zero wear of the sample surface and also eliminated postdata analysis errors in surface feature height scratch/wear tests were performed over a scan area of 2 × 2 μm^2 at a scan rate of 10 Hz. The reported scratch/wear depths are an average of six runs at separate instances. In this study, all of the measurements were carried out in ambient conditions (22°C, RH 40–44%).

RESULTS AND DISCUSSION

Characterization of the prepared films

Figure 2 shows a series of AFM images taken over regions 1.0 × 1.0 μm^2 of specimens at various stages of the film deposition process, where (a) refers to the bare cleaned silicon substrate; (b) APTES-SAM on the silicon substrates; (c) to the phosphorylated APTES-SAM; (d) to the as-deposited thin films on the phosphorylated APTES-SAM. It is seen that the surface of the silicon substrates [Fig. 2(a)] is clean and smooth with surface root-mean-square (rms) roughness in the range of 0.2–0.3 nm. [Fig. 2(b)] is uniform and homogenous with surface rms roughness about 0.522 nm. The phosphorylated APTES-SAM [Fig. 2(c)] becomes more and more uniform and homogeneous with rms roughness about 0.393 nm. The possible reason is that the size of $-PO(OH)_2$ groups is bigger than the terminal groups $-NH_2$ which leads to the $-PO(OH)_2$ terminal molecules provided a more densely packed arrangement than the $-NH_2$ terminal molecules. After the deposition of the thin films [Fig. 2(d)] on the phosphorylated APTES-SAM, many differences are visible in the corresponding AFM images. Namely,

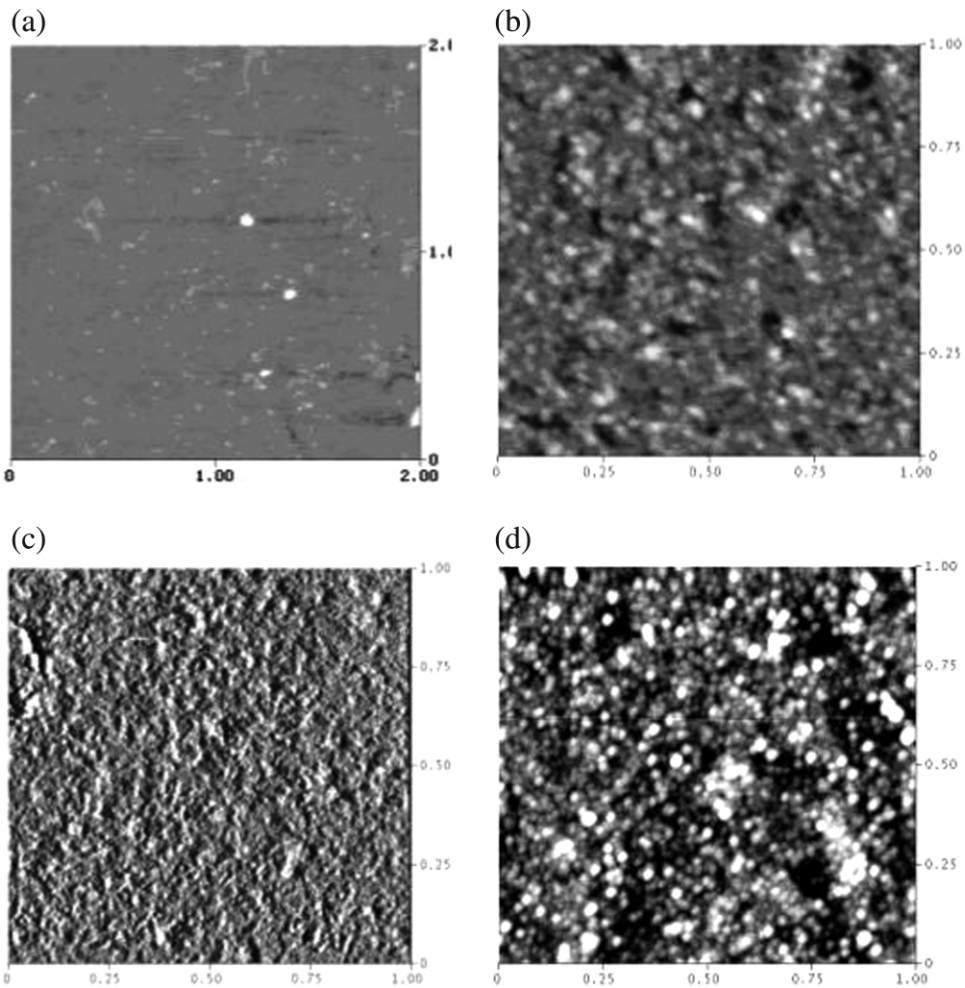

Figure 2 (a) AFM images of the surface of the bare cleaned silicon substrate; (b) AFM images of the surface of APTES-SAM on the silicon substrate; (c) AFM images of the surface of the phosphorylated APTES-SAM; (d) AFM images of the surface of the as-deposited thin films on the phosphorylated APTES-SAM.

the surface of the as-deposited films is rough and quite densely round-looking particles with the rms roughness to be about 0.863 nm, which shows wide potential application in lubrication and wear protection.

The XPS spectra applied to detect the chemical states of some typical elements for the prepared films are shown in Figures 3–6. XPS survey and single scan spectra of APTES-SAM (seen in Fig. 3) shows contributions from the substrate and the film in at %: silicon (15.5%), carbon (56.3%), oxygen (20.2%), and nitrogen (8.0%). Nitrogen is detected which indicates successful APTES-SAM deposition, since this element is only contained in this film material. Figure 4 shows single-scan XPS spectra of N 1s peak decomposed into two different nitrogen species occurring in different binding states. The peak at 400.8 eV is assigned to the protonated aliphatic amino groups, whereas that at 399.5

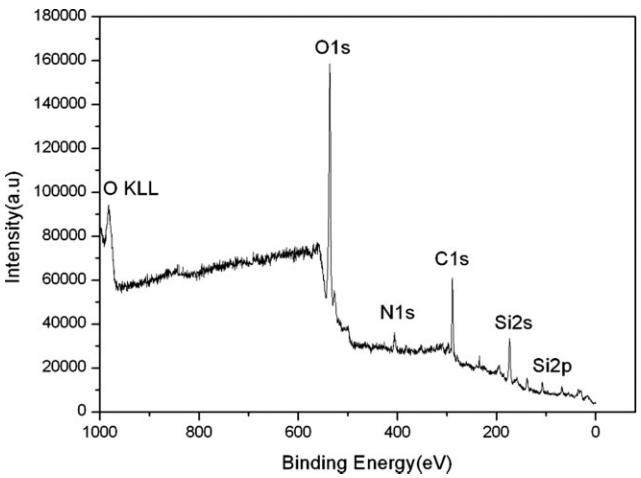

Figure 3 XPS survey and single scan spectra of APTES film.

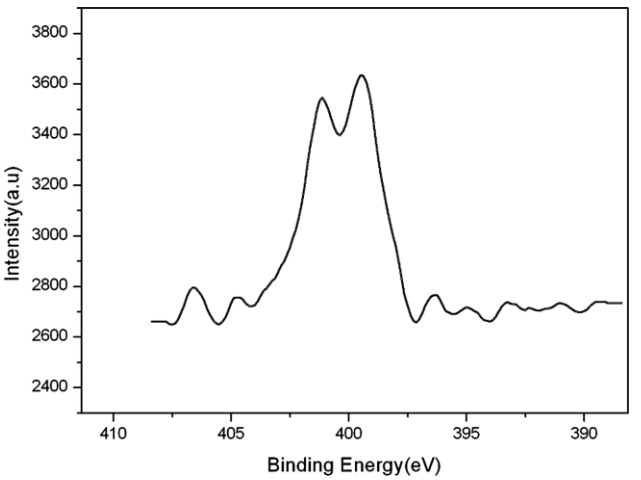

Figure 4 Single scan XPS spectrum of the N 1s region of an APTMS film.

eV may be ascribed to the aliphatic amino groups. This interpretation is consistent with Ref. 18.

After *in situ* phosphorylation of the APTES-SAM, the P 2p at 134.5 eV is observed (Fig. 5), which is assigned to the P atoms in $-PO(OH)_2$ group and N signal is absent. It indicates that the terminal $-NH_2$ group in the APTES-SAM has been phosphorylated and transformed to $-PO(OH)_2$ group successfully and completely.

The contact angles of distilled water on silicon substrate and the prepared films were measured using a contact angle measurement. The APTES-SAM has a contact angle of $50^\circ \pm 2^\circ$, which is consistent with a moderately polar surface where the amino group is oriented upward. After phosphorylated *in situ* for 20 min, a contact angle of $24^\circ \pm 2^\circ$ is recorded for the phosphorylated surface. The contact angle of thin films deposited on the phosphorylated APTES-SAM increases to $66^\circ \pm 2^\circ$. The change of the contact angles means the film has been prepared on the silicon substrate. So the surface with different contact angles has different surface properties.

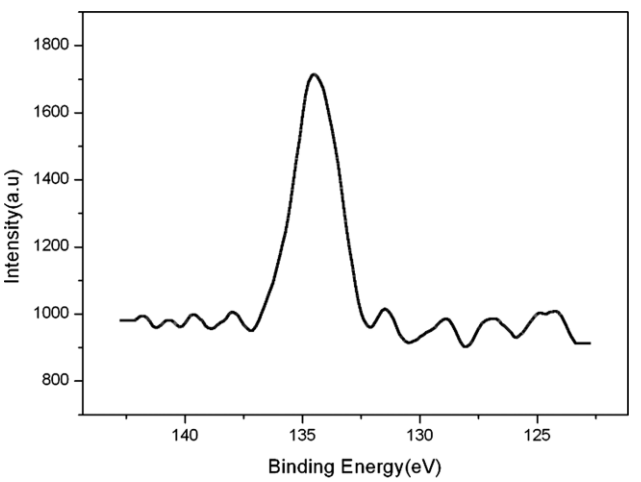

Figure 5 Single scan XPS spectrum of the P 2p region in APTMS film.

In our work, the thickness of the prepared films on glass substrates is determined with ellipsometer. The averaged thickness of the APTES-SAM is about 7.5 nm, which matches with the projection of a normally extended molecular chain on the surface. The thickness is hardly changed after the $-NH_2$ is phosphorylated to $-PO(OH)_2$ group, which indicates that a monolayer of phosphorylated APTES has been prepared on glass substrates. The thickness increases about to 15 nm after the phosphorylated APTES-SAM is immersed in solution, which also shows that thin films have been successfully obtained.

Nanotribological properties of the prepared films

Adhesion, friction, and work of adhesion

Figure 6 shows the average values of the adhesion force and coefficients of friction of four kinds of flat surfaces measured by contact mode AFM under an applied normal load of 20 nN and a scan rate of

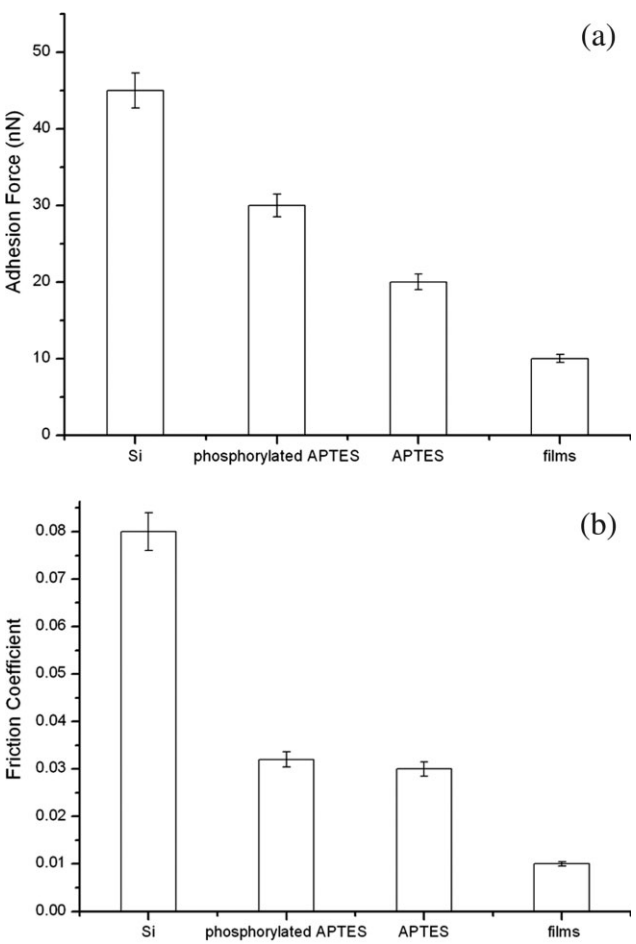

Figure 6 (a) Adhesive forces of silicon and the prepared films; (b) Coefficients of friction of silicon and the prepared films.

10 Hz. It shows that SAMs can reduce the adhesive and frictional forces of silicon substrate. In particular, thin films exhibit the lowest adhesive force and coefficient of friction. It means that the prepared films can be used as effective molecular lubricants for micro/nanodevices fabricated from silicon. Based on the data, the ranking of adhesive forces F_a is in the following order: $F_{a\text{-Si}} > F_{a\text{-phosphorylated APTES}} > F_{a\text{-APTE}} > F_{a\text{-films}}$. And the ranking of the coefficients of friction is in the following order: $\mu_{Si} > \mu_{\text{phosphorylated APTES}} \approx \mu_{\text{APTES}} > \mu_{\text{films}}$.

Based on Young-Dupre equation, work of adhesion W_a [the work required to pull apart the unit area of the solid interface, eq. (1)[19]] was summarized:

$$W_a = \gamma_{1a}(1 + \cos\theta_1) \quad (1)$$

Where γ_{1a} is the surface tension of liquid-air interface and θ_1 is the water contact angle of liquid and flat. From Figures 6 and 7, it was found that the adhesive force and friction coefficient decreases as the work of adhesion decreases. It implies that the capillary force acting between the tip and the flat surfaces affected seriously on nanoadhesion and nanofriction. From Figure 6, it can be also found that APTES-SAM and phosphorylated APTES-SAM have polar surface groups (—NH_2 and —$PO(OH)_2$ groups), thus lead to larger W_a and eventually larger adhesive forces. The films do not have polar surface groups, thus have a smaller W_a and adhesive force than APTES-SAM and phosphorylated APTES-SAM.

Scratch/wear tests

As explained earlier, the scratch tests of silicon and the prepared films were studied by making scratches for 10 cycles with varying loads. Figure 8 shows a plot of scratch depth versus normal load for various samples. Scratch depth increases with increasing normal load. APTES-SAM and phosphorylated APTES-SAM show similar scratch resistance. From the data, it is clear that the thin films show the best scratch resistance compared with the silicon substrate, APTES-SAM and phosphorylated APTES-SAM. The increase in scratch depth with normal load is very small and all depths are <20 nm, whereas the silicon substrate and APTES-SAM finally reach depths of about 80 and 150 nm, respectively.

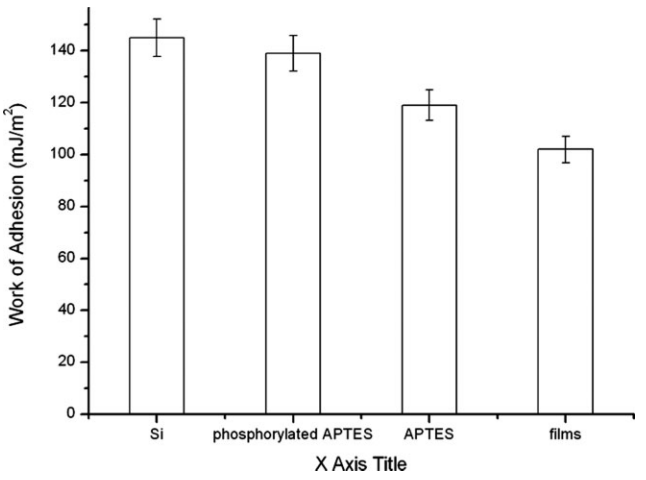

Figure 7 Work of adhesion of friction of silicon and the prepared films.

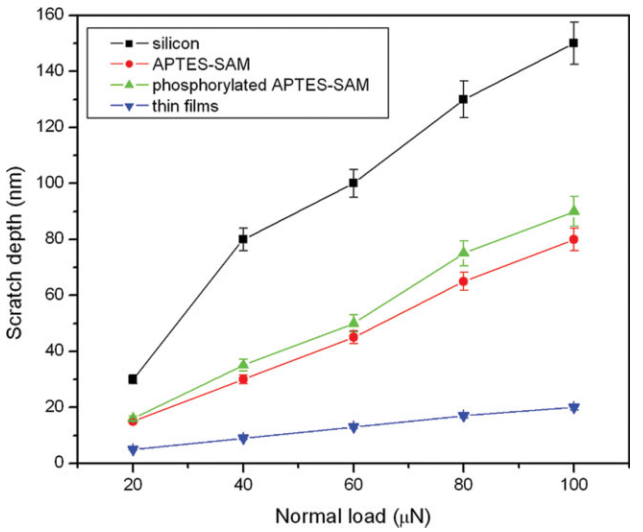

Figure 8 Scratch depths for 10 cycles as a function of normal load. [Color figure can be viewed in the online issue, which is available at www.interscience.wiley.com.]

Wear tests were conducted on the samples by wearing the same region for 30 cycle at a normal load of 20 μN, while observing wear depths at different intervals (1, 5, 15, 20, and 30 cycles). This would give

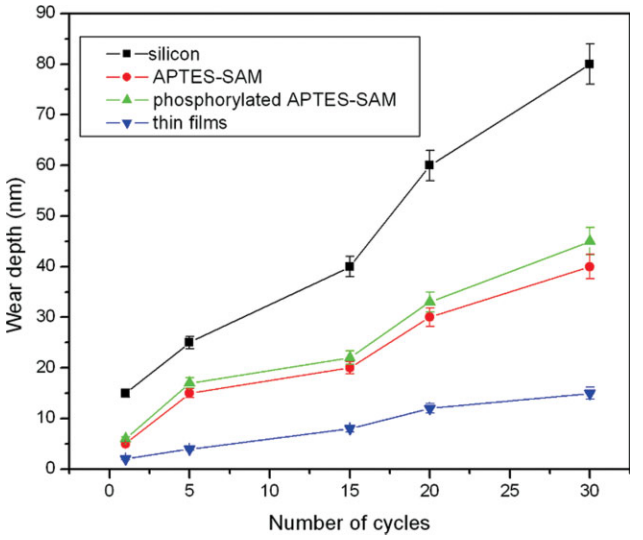

Figure 9 Wear depths as a function of number of cycles. [Color figure can be viewed in the online issue, which is available at www.interscience.wiley.com.]

information as to the progression of wear of the films. The wear depths observed are plotted against number of cycles in Figure 9. For all the samples, the wear depth increases almost linearly with increasing number of cycles. This suggests that material is removed layer by layer in all the materials. Here also, thin films exhibit lesser increase in wear depth (slope) than the other samples. APTES-SAM wears less than the silicon substrate, which shows similar wear characteristics to the phosphorylated APTES-SAM. Combined with the scratch/wear data and the thickness of the films, it can be found that the scratch/wear depth of APTES-SAM and phosphorylated APTES-SAM are much more than their thickness (7.5 nm). On the contrary, the scratch/wear depth of thin films does not exceed its thickness (15 nm) all the time. It shows that APTES-SAM and phosphorylated APTES-SAM are seriously destroyed with the increase of normal load and number of cycles, whereas thin films are still not completely worn at last. The scratch/wear results all indicate that thin films have better surface mechanical properties than silicon substrate, APTES-SAM, and phosphorylated APTES-SAM.

The $-PO(OH)_2$ group on the APTES-SAM provides net negative charge, thus promoting the process of self-assembly. Then $-PO(OH)_2$ can provide a P=O bond as complexing group to react after adsorption, thus improving the bonding strength between the films and the silicon substrates. In addition, Hertzian cone cracks can occur when the normal stress exceeds a critical value as the AFM tip slides over the surface. Friction forces during sliding reduce this critical value. In a word, strong bonding strength between the films and the silicon substrate and low coefficient of friction are responsible for the superior scratch/wear resistance of thin films.

CONCLUSIONS

In this work, the nanotribological properties of silicon substrate, APTES-SAM, phosphorylated APTES-SAM, and the thin films were characterized by an AFM. The thin films showed the lowest friction and adhesion followed by APTES-SAM and phosphorylated APTES-SAM, whereas silicon substrate showed high friction and adhesion. Microscale scratch/wear studies clearly showed that thin films were much more scratch/wear resistant than the other samples. The superior friction reduction and scratch/wear resistance of thin films may be attributed to low work of adhesion of nonpolar terminal groups and the strong bonding strength between the films and the substrate.

It is thus concluded the prepared thin films could be used for protection from scratching as well as reducing friction.

References

1. Anonymous. Microelectromechanical Systems: Advanced Materials and Fabrication Methods, NMAB-483; National Academy Press: Washington, DC, 1977.
2. Roukes, M. Phys World 2001, 14, 25.
3. Bhushan, B. Tribology Issues and Opportunities in Mems; Kluwer Academic: Dordrecht, Netherlands, 1998.
4. Bhushian, B. Handbook of Micro/Nanotribology, 2nd ed.; CRC: Boca Raton, FL, 1999.
5. Kayali, S.; Lawton, R.; Smith, B. H.; Irwin, L. W. EEE Links 1999, 5, 10.
6. Arney, S. MRS Bull 2001, 26, 296.
7. Bhushan, B.; Israelachvili, J. N.; Landmann, U. Nature 1995, 374, 607.
8. Dugger, M. T.; Senft, D. C.; Nelso, G. C. ACS Symp Ser 2000, 741, 455.
9. Depalma, V.; Tillman, N. Langmuir 1989, 5, 868.
10. Tsukruk, V. V.; Bliznyuk, V. N.; Hazel, J.; Visser, D.; Everson, M. P. Langmuir 1996, 12, 4840.
11. Boshui, C.; Yi, Y.; Junxiu, D. J Chin Rare Earth Soc 1998, 16, 220.
12. Cha, K. H.; Kim, D. E. Wear 2001, 251, 1169.
13. Bhushan, B. Wear 2005, 259, 1507.
14. Buscher, C. T.; McBranch, D.; DeQuan, L. J Am Soc 1996, 118, 2950.
15. Katz, H. E.; Scheller, G.; Putvinski, T. M.; Schilling, M. L.; Wilson, W. L.; Chidsey, C. E. D. Science 1991, 254, 1485.
16. Binnig, G.; Quate, C. F.; Gerber, Ch. Phys Rev Lett 1986, 56, 930.
17. Glosli, J. N.; McClelland, G. M. Phys Rev Lett 1993, 70, 1960.
18. Bierbaum, K.; Kinzler, M.; Wöll, Ch.; Gruzne, M.; Hähner, G.; Heid, S.; Effenberger, F. Langmuir 1995, 11, 512.
19. Israelachvili, J. N. Intermolecular and Surface Forces; Academic Press: New York, 1985.